Research Article

Current Research in Statistics & Mathematics

How Can we Observe Waves Without Seeing the Ocean? the Witte-Ulianov Time Interferometer: A Gravitational-Wave Detector Without a Lower Frequency Limit

Policarpo Yōshin Ulianov*

***Corresponding Author**
Policarpo Yōshin Ulianov

Submitted: 2023, Sep 07 ; **Accepted:** 2023, Oct 02 ; **Published:** 2023, Oct 11

Citation: Ulianov, P. Y. (2023). How Can we Observe Waves Without Seeing the Ocean? the Witte-Ulianov Time Interferometer: A Gravitational-Wave Detector Without a Lower Frequency Limit. *Curr Res Stat Math, 2*(1), 56-70.

Abstract

This article introduces the Witte-Ulianov Time Interferometer (WUTI), a pioneering gravitational-wave (GW) detector. Built upon Einstein's General Relativity (GR), WUTI capitalizes on the concept that gravitational fields can influence time dilation, akin to a "time flow rate" or "time velocity."

In February 2016, the Laser Interferometer Gravitational-Wave Observatory (LIGO) made history by detecting a gravitational wave. However, LIGO's detectors are hampered by technical limitations, particularly low-frequency noise sources, confining their measurement range to 80-300 Hz. This narrow span is incongruous with major events that can generate GWs spanning seconds to hours. Analogously, LIGO offers a glimpse of a universe observed through gravitational waves, though it's akin to peering through a "keyhole" rather than unlocking this new universe's full potential.

The Witte-Ulianov Time Interferometer identifies gravitational waves through time distortion, as predicted by General Relativity when these waves traverse the detector. WUTI employs the Witte effect, first noted by R. D. Witte in 1991 while measuring disparities between atomic clocks. This effect facilitates observing time distortions by assessing phase changes across precise time sources.

The Witte effect enables the measurement of "time flow" alterations between two points in space, utilizing accurate time sources like atomic clocks or highly stable frequency laser sources. Upon encountering a gravitational wave, these clocks experience modified "time flow" between them, observable through phase comparators.

WUTI's operation is minimally affected by physical phenomena, unlike LIGO detectors susceptible to numerous noise sources, particularly at low frequencies. While WUTI's time sources may face external influences like temperature changes, the devised method uses a dual-phase comparison that inherently eliminates errors within time sources. This approach subtracts two practically identical phase errors, effectively canceling them out—except when the time flow changes momentarily, such as a gravitational wave's arrival that impacts each source individually, generating phase discrepancies in the phase detector.

As a result, the WUTI detector operates without low-frequency limitations, capable of detecting gravitational waves with periods ranging from seconds to hours. This enables the detection of slow gravitational field variations, facilitating the observation of Earth's field fluctuations due to its movement and rotation. WUTI can observe gravitational fields of the moon, sun, and Milky Way, uncovering not just gravitational waves, but also the "Gravity Ocean" Earth traverses.

Keywords: Gravitational waves, LIGO, Laser Interferometer Gravitational-Wave Observatory.

1. Introduction

On September 13th, 2015, a groundbreaking announcement was made: The Laser Interferometer Gravitational-Wave Observatory (LIGO) had detected its first gravitational wave event, named GW150914 [1]. This landmark discovery, celebrated as a triumph by the hundreds of physicists at LIGO, marked the observation of gravitational waves generated by the collision of black holes.

However, amidst this celebratory atmosphere, certain authors have raised the possibility that LIGO's detection might be a false alarm. The signals recorded from the GW150914 event, as depicted in Figure 1, are linked to gravitational waves arising from black hole collisions [2, 3].

While this discovery heralded a new era in gravitational wave astronomy, LIGO's detection process is not without limitations. The apparatus's ability to detect gravitational waves is confined within a narrow frequency range, specifically from 80 to 300 Hz. Given the astronomical events capable of generating gravitational waves with periods spanning seconds to hours, this frequency range appears notably restrictive.

In the GW150914 event, the recorded signals exhibit a duration of less than 0.1 seconds, as evidenced in Figure 1. For further illustration, Figure 2 portrays the "NF waveform" (in green) representing Numerical Relativity signal—a simulation of the black hole collision—spanning a few seconds. A direct comparison of signals in Figure 2 reveals that LIGO's detectors missed capturing the initial phases of the gravitational wave curves due to the limitations of their low-frequency range.

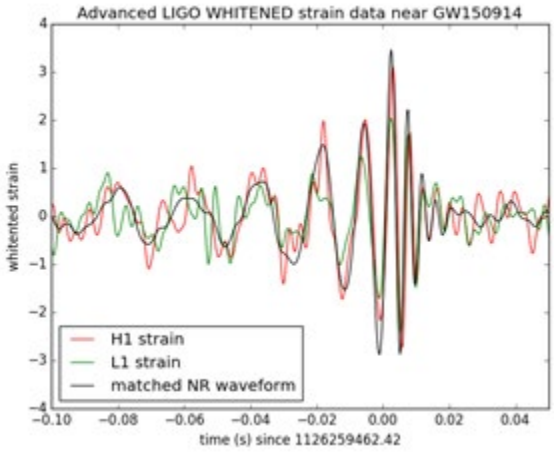

Figure 1: *Processed signals from the GW150914 event*

Had LIGO possessed a broader frequency range, such as 10 to 300 Hz, both signals in Figure 2 would present identical shapes, eliminating any doubt about the occurrence of gravitational waves during this event. This would enable immediate recognition that the recorded signals indeed originated from a collision involving two black holes.

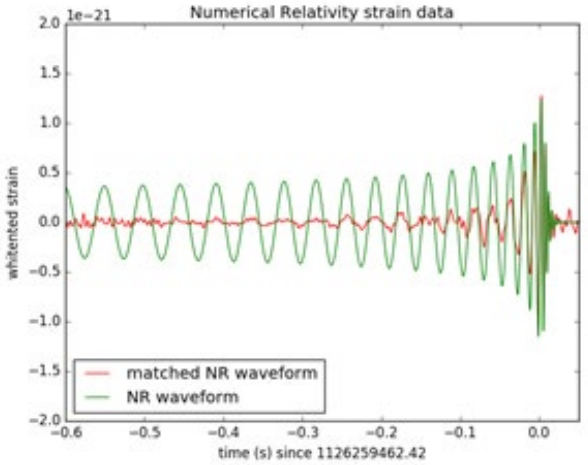

Figure 2: *Signals from the black hole collision: NR waveform in green and matched NR waveform in red. Both graphs depict the same curves across varying time windows.*

2. LIGO Gravitational Wave Detection:

Einstein's General Relativity (GR) theory postulates that gravitational waves induce distortions in space-time. LIGO's approach revolves around detecting these distortions via a modified Michelson interferometer. This entails recording gravitational wave signals by gauging the length difference in the interferometer's orthogonal arms.

Within LIGO detectors, each arm integrates two mirrors functioning as test masses. A passing gravitational wave alters the lengths of these arms, a variation measurable through the interference of laser beams—a fundamental principle behind Michelson interferometry.

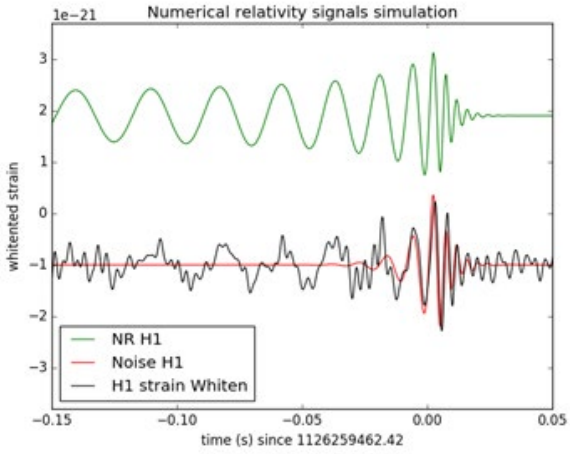

Figure 3: *Signal from the black hole collision: NR waveform (in green),noise signal (in red), and recorded strain at Hanford (in black)*

However, the challenge lies in this "space distortion" detection methodology. Various factors can trigger movements in the test mass, which consequently infuses substantial noise into the interferometer output. Regrettably, this amplified noise profoundly restricts LIGO's measurement frequency range, confining it between 80 and 300 Hz.

A significant drawback of this limitation is apparent when a genuine gravitational wave signal intersects with noise, as depicted in Figure 3. The H1 strain (black signal) may stem from either a black hole collision (green signal) or random noise (red signal). As such, solely examining the H1 strain curve doesn't allow differentiation between a legitimate event and a spurious noise occurrence.

Consequently, LIGO utilizes two detectors, Hanford and Livingston, to discern genuine gravitational waves from noise. For instance, the GW150914 event (Figure 1) showcases similar waveforms, recorded with a 7.5 ms time discrepancy. This time gap resides within a 10 ms time window, which signifies the maximum time light requires to traverse between both detectors. Therefore, the signals captured in the GW150914 event might signify the same gravitational wave sequentially striking both detectors.

Nonetheless, this alignment doesn't dismiss the possibility that the recorded GW150914 signals could merely be two coincidental noises coinciding within the same time window. To address this, the LIGO team conducted a statistical analysis, deducing that this form of coincidence could materialize once every 67 thousand years.

In light of the frequency range limitations in LIGO's detectors, this author posits that the system transforms from a "general gravitational-wave detector" into a "Black Hole Collision

detector," necessitating several months or years before a new event can be detected.

An analogy with oceanic waves provides insight—LIGO resembles a Tsunami detector, activated over extended periods but incapable of perceiving the multitude of waves incessantly striking the shore.

3. Witte-Ulianov Time Interferometer:

The Witte-Ulianov Time Interferometer fundamentally observes gravitational waves by leveraging the phenomenon of time distortion that, according to General Relativity (GR), manifests when these waves interact with Earth. Central to this novel interferometer's functionality is the Witte effect, first discovered by R. D. Witte in 1991 while employing phase comparison techniques to rectify errors in atomic clocks.

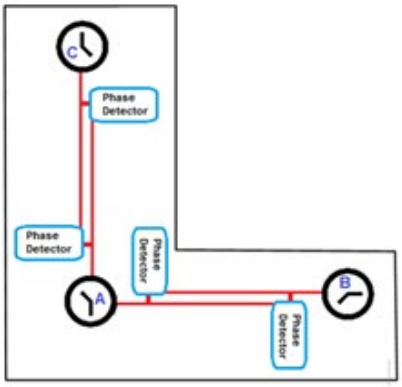

Figure 4: *White-Ulianov Time Interferometer with two arms*

Remarkably, the Witte effect, which is explored in greater detail subsequently in this article, facilitates the measurement of Earth's velocity in space—an aspect that contemporary physicists have not universally acknowledged. This intriguing outcome aligns with Michelson's original expectations when devising his interferometer. Michelson's experiment, however, encountered a shortfall due to Special Relativity's revelation that the interferometer arm lengths shift in response to Earth's displacement and rotation. Consequently, the measured speed of light via Michelson's interferometer remains invariant, failing to register the addition or subtraction of Earth's velocity to the speed of light.

This author contends that the Witte effect holds the capacity to detect alterations in Michelson's interferometer arm lengths because this variability stems from space contraction—a phenomenon intrinsically tied to time dilation. Space contraction emerges through two avenues:

• In accordance with Special Relativity, observers moving at significant velocities experience a slower "flow" of time, and objects contract along their trajectory.
• General Relativity stipulates that gravitational fields also trigger a deceleration of time flow and a contraction of space for observers within them.

Hence, the gravitational waves effectively reshaping LIGO's interferometer arm lengths also engender changes in time flow between points positioned at the arms' termini and the junction point.

Figure 4 presents a fundamental two-arm Witte-Ulianov Time Interferometer, readily adaptable onto the existing LIGO structure. Notably, the clocks depicted can encompass atomic clocks, employing coaxial cables or microwave conductors connected via electronic circuits for phase change detection. To heighten temporal precision, stable laser sources producing light beams can be utilized, with direct phase detection achieved through photodetectors. Optical fiber cables can facilitate connections between laser sources and phase detectors, although the optimal approach involves exploiting the vacuum chambers present in contemporary LIGO detectors.

Importantly, the WUTI gravitational-wave detector captures two phase shift signals, with each signal proportionate to the gravitational-wave projection onto the corresponding arm. Furthermore, the WUTI gravitational-wave detector is amenable to a three-arm configuration, encompassing a third arm mounted atop a towering structure or within a subterranean well.

4. The Witte Effect:

Discovered by R. D. Witte in 1991 through a 177-day experiment, the Witte effect emerged as a significant phenomenon. Witte's experiment involved monitoring the phase delays between atomic clocks connected by a 1.5 km length coaxial cable [4].

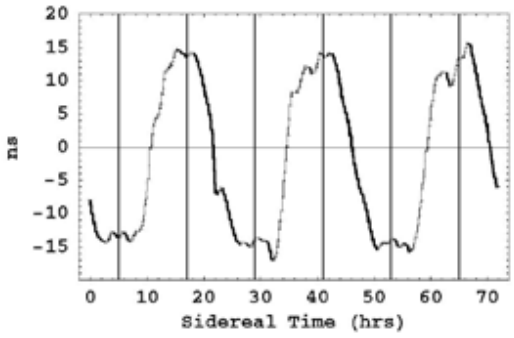

Figure 5: Phase drifts, as observed by Roland De Witte in 1991

Figure 5 presents Witte's recorded phase delays spanning three consecutive days. Evidently, a sinusoidal variation in phase delay is discernible, characterized by a period closely mirroring the sidereal day.

The amplitude of this sinusoidal variation, symbolized by the value Δt, is calculated via the following equation:

$$\Delta t = L\frac{v_E n^2}{c^2} \qquad (1)$$

Here, L signifies the cable length, n represents the cable's refractive index, and c denotes the speed of light in a vacuum. Notably, the speed v_E is intrinsically connected to Earth's velocity during its journey through space.

Witte's experimental results faced a roadblock in publication due to their apparent contradiction with Special Relativity. Only in 2006 did the Witte effect gain acknowledgment as genuine,

when R. T. Cahill [2] proposed an explanation that harmonized with Einstein's principles of relativity without generating contradictions.

5. Rotating Einstein's Light Clock to Explain the Witte Effect:

The Witte Effect finds a clear explanation through the rotation of Einstein's light clock [3]. Figure 6 presents the fundamental concept of Einstein's light clock, a quintessential example illustrating relativistic time dilation.

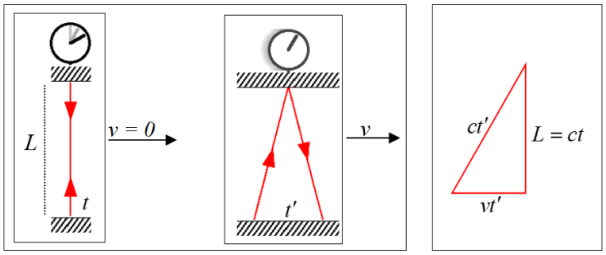

Figure 6: *Einstein's light clock*

From the triangle depicted in Figure 6, the following equations can be deduced:

$$(ct')^2 = (ct)^2 + (vt')^2$$

$$t'^2\left(1 - \frac{v^2}{c^2}\right) = t^2$$

$$t' = t\frac{1}{\sqrt{1 - \frac{v^2}{c^2}}} \quad \rightarrow \quad t' = tY \qquad (2)$$

$$Y = \frac{1}{\sqrt{1 - \frac{v^2}{c^2}}} \qquad (3)$$

To analyze Einstein's light clock rotation, let's imagine two of Einstein's light clocks in a 90-degree configuration within a moving room in space, as shown in Figure 7. A vacuum exists inside the clock room, where light beams propagate at the speed of light (c). If the room is stationary, it forms a square. However, when moving at speed v, the room shrinks according to its movement direction.

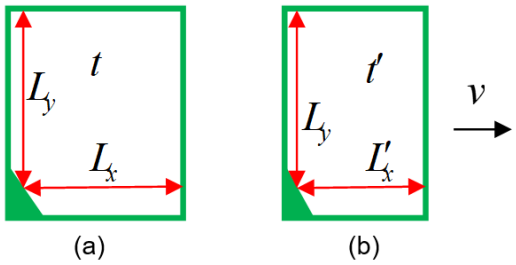

Figure 7: *Two of Einstein's light clocks: a) room stationary; b) room moving at speed v.*

The dual clock setup in Figure 7 can be observed through sequences of time, as presented in Figure 8. This involves considering two scenarios: with the clock stationary and with the clock moving at speed v. In the stationary case, two light pulses travel within the room during time frames (t_0,t_1,t_2,t_3,t_4). These pulses essentially have the same movement, going out and returning simultaneously. In the case of the room moving, an external observer witnesses the light pulse in the horizontal path moving at the speed of light, while the room wall is simultaneously moving at speed v. As a result, the vertical light pulse hits the top of the room at time t_2^' before the horizontal pulse hits the right wall. Conversely, when the horizontal light pulse returns, the relative speed (considering the wall and the light pulse) slightly exceeds the speed of light (c + v), causing both pulses to arrive simultaneously.An observer within the room always experiences the stationary case, unable to detect room contraction or perceive fluctuations in the speed of light pulses.

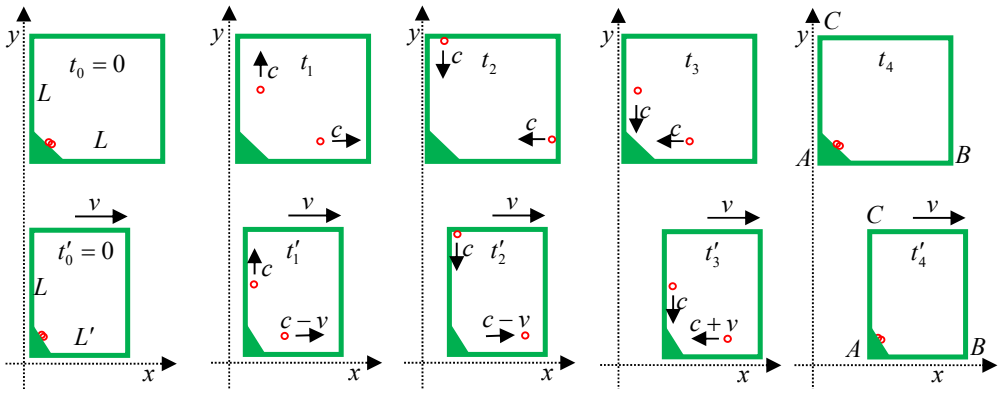

Figure 8: *Time frames for the rooms presented in Figure 8.*

Figure 9 demonstrates Einstein's light clock, designed to rotate while in motion. For a comprehensive grasp of its functioning, two precision atomic clocks are utilized—one at each end of the light clock. These clocks, perfectly in sync, are governed by the "hits" of light.

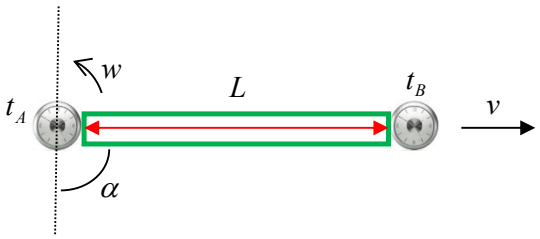

Figure 9: *Rotating the Einstein's light clock.*

In scrutinizing the rotation of Einstein's light clock as depicted in Figure 9, one can envision two instances: when α equals zero and 90 degrees. The clock designated as "A" remains stationary, thus rendering its measured time t'_A impervious to rotation. On the contrary, clock "B" undergoes a 90-degree rotation around clock "A," resulting in clock "B" measuring time t'_A, contingent upon angle α. Consequently, the rotating Einstein's light clock begets a temporal propagation delay (t'_{AB}) contingent on α:

$$t'_B(\alpha) = t'_A + t'_{AB}(\alpha)$$
$$t'_{AB}(\alpha) = t'_B(\alpha) - t'_A \qquad (4)$$

Equations (2) and (3) then permit us to define a phase delay (t_AB^') linked to temporal disparities. This delay can be calculated through:

$$t'_{AB}(\alpha) = \sqrt{\left(Y^2 \frac{L'}{c}(1-\frac{v}{c})\right)^2 sin^2(\alpha) + \left(\frac{L'}{c}\right)^2 cos^2(\alpha)} \qquad (5)$$

It is vital to highlight that in Equation (5), the intricacies of time disparities necessitate the utilization of a squared metric for temporal distance computation—a reflection of how time operates analogously to spatial dimensions within the context of Special Relativity.

For an observer within the room, Equation (5) reduces to:

$$t_{AB}(\alpha) = \frac{t'_{AB}(\alpha)}{Y}; L = YL';$$
$$t_{AB}(\alpha) = \frac{L}{c} - \frac{vL}{c^2} sin(\alpha) \qquad (6)$$

Hence, a variation in the time propagation delay (*tAB*) is defined:

$$t_{AB}(\alpha) = \frac{L}{c} - \Delta t_{AB}(\alpha)$$
$$\Delta t_{AB}(\alpha) = L\frac{v}{c^2} sin(\alpha) \qquad (7)$$

This signifies that by rotating Einstein's light clock (Figure 7), a discernible variation in the phase delay (Δt_AB) emerges between the two clocks. Remarkably, when α equals 90 degrees, Equation (7) calculates a time propagation delay analogous to the Witte effect, quantified by Equation (1). The refraction index present in Equation (1) is excluded from Equation (7) due to Einstein's light clock operating within a vacuum.

For an Earth-based implementation of the experiment in Figure 7, the angle α fluctuates with sidereal time, generating a sinusoidal waveform as described in Equation (7). R. D. Witte's experiment—employing two atomic clocks placed kilometers apart—generated synchronized sine waves across a coaxial cable, compared through a phase shift meter. This experiment yielded a sine wave delay with a 15 ns amplitude and a sidereal time period, as represented in Figure 1. Using this value—attributed to the clocks' distance and speed—R. D. Witte calculated Earth's velocity in space.

This phenomenon, acknowledged as the Witte effect, finds its explanation through the rotation of Einstein's light clock. Moreover, considering Earth's motion relative to the Cosmic Microwave Background, its velocity approximates 369 km/s. By employing a Witte-Ulianov Time Interferometer with an L value of 4 km, a time delay—according to Equation (7)—amounts to 16.2 ns.

6. Witte Effect Over Gravitational Fields:

When applying the GR field equations to the scenario of a single spherical mass M in empty space, it leads to a solution known as the Schwarzschild metric [4]. This metric can be defined in spherical coordinates by the Schwarzschild equation:

$$ds^2 = c^2(1-\frac{2GM}{c^2 r})dt^2 - \frac{dr^2}{1-\frac{2GM}{c^2 r}} - r^2 d\Omega^2$$
$$d\Omega^2 = d\theta^2 + \sin^2(\theta)\, d\phi^2 \qquad (8)$$

Where (r, θ, ϕ) represent points in a spherical coordinate system centred at the gravity center of the spherical mass.

For an observer far from the mass, Equation (8) is simplified to:

$$ds^2 = c^2 dt^2 - dr^2 - r^2 d\Omega^2 \qquad (9)$$

For an observer near the mass, at a specific distance r, the displacement ds^'2 can be defined as:

$$ds'^2 = c^2(1-\frac{2GM}{c^2 r})dt'^2 - \frac{dr'^2}{1-\frac{2GM}{c^2 r}} - r^2 d\Omega'^2 \qquad (10)$$

Comparing Equations (14) and (15), the time dilation effect predicted by the Schwarzschild equation can be calculated as:

$$c^2 dt^2 = c^2(1-\frac{2GM}{c^2 r})dt'^2$$
$$t' = t\frac{1}{\sqrt{1-\frac{2GM}{c^2 r}}} \qquad (11)$$

Comparing this to Equation (2), a time dilation equivalence can be observed:

$$t' = t\frac{1}{\sqrt{1-\frac{v^2}{c^2}}} \;;\; t' = t\frac{1}{\sqrt{1-\frac{2GM}{c^2 r}}}$$
$$v^2 = \frac{2GM}{r}$$
$$v = \sqrt{\frac{2GM}{r}} \qquad (12)$$

This equivalence allows us to recreate the rotating Einstein's light clock experiment depicted in Figure 7, now considering that the system's velocity is negligible and that the two clocks are at a distance r from a mass M, as illustrated in Figure 10.

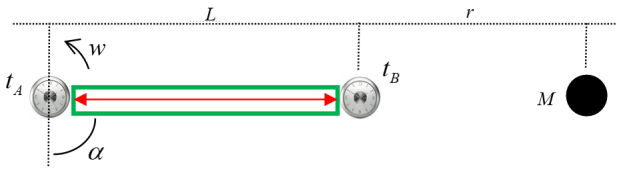

Figure 10: *Rotating the Einstein's light clock near a spherical mass M.*

Since the experiments in Figure 7 and Figure 10 have equivalent time dilation effects, using equations (7) and (12), we can derive the Witte effect applied to gravitational time distortions when rotating clocks over a gravitational field, with consideration for the angle α defined in Figure 10:

$$\Delta t_{AB}(\alpha) = \frac{L}{c^2}\sqrt{\frac{2GM}{r}}\sin(\alpha) \qquad (13)$$

In the setup shown in Figure 10, the time distortion in clock A is assumed to be constant. Consequently, as clock B orbits around clock A, the time distortion over clock B will change as a function of angle α, as described by equation (13).

By applying equation (13) to the moon's mass (7.6×10^{22} kg) and its distance from Earth (3.8×10^{8} m) with an L value of 4 km, the maximum time variation is approximately 7.1 picoseconds. Similarly, for the sun's mass (1.99×10^{30} kg) and its distance from Earth (1.49×10^{11} m) with an L value of 4 km, the maximum time variation is around 1.8 ns.

This implies that with two highly precise clocks, featuring a time resolution on the order of 0.1 picoseconds (clock frequency of 10 GHz), and the ability to compare time differences with this level of precision, it would be feasible to not only detect gravitational waves but also identify the Witte Effect. This effect could be generated by Earth's rotation in the presence of the moon's gravitational field, as well as by the clock's time being affected by the sun's gravitational field.

7. WUTI Implementation Using Atomic Clocks:

Figure 11 illustrates the foundational configuration of the Witte-Ulianov Time Interferometer (WUTI) with a single-arm design. In this arrangement, a pair of atomic clocks plays a pivotal role as reference points for time measurement. The frequencies emitted by each atomic clock undergo a division process, which in turn orchestrates the synchronization of a sine wave generator (SG). This SG operates at a significantly "lower" frequency compared to the clock's GHz frequency, typically around 10 MHz or 100 MHz. Despite its lower operational frequency, the SG generates a sine wave signal, characterized by its phase being intricately synchronized with the current time of the respective atomic clock.

As a consequence of this synchronization, the analog sine wave signal effectively carries intricate high-precision digital time information. The resulting output signal from each SG travels through coaxial cables, eventually reaching and interfacing with two phase comparators (PCs).

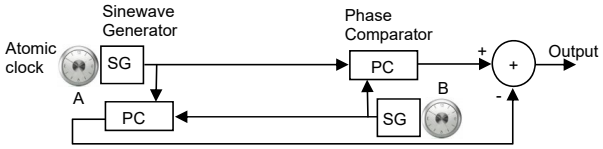

Figure 11: *WUIT implementation using atomic clocks.*

In the presented configuration (Figure 11), every phase comparator (PC) receives two sine wave signals: one originating locally and the other remotely. Ideally, both atomic clocks would register the same time, resulting in null outputs from the phase comparators. However, in practical scenarios, various factors such as temperature fluctuations introduce operational deviations. These deviations can be modeled as error signals, which are then added to the ideal time ($t_{ClockX} = t + e_X$).

When the sine wave generators (SGs) function at angular frequencies denoted as w_A and w_B, their output signals adhere to the following equations:

$$S_A(t) = V_A \sin(w_A(t + e_A) + \varphi_A) \qquad (14)$$
$$S_B(t) = V_B \sin(w_B(t + e_B) + \varphi_B) \qquad (15)$$

Accounting for the cable delay in signal transmission between points X and Y, each phase comparator processes signals as defined by equations (19) and (20). The cable delay is represented as Δt_AB for the signal from point A to point B and Δt_BA for the reverse direction. Calculations proceed as follows:

Accounting for the cable delay in signal transmission between points X and Y, each phase comparator processes signals as defined by equations (19) and (20). The cable delay is represented as Δt_AB for the signal from point A to point B and Δt_BA for the reverse direction. Calculations proceed as follows:

P_A(t) = PhaseCompare[S_A(t), S_B(t + Δt_BA)]
P_A(t) = w_A * t + w_A * e_A + φ_A - w_B * t - w_B * Δt_BA - w_B * e_B - φ_B

(21)

P_B(t) = PhaseCompare[S_A(t + Δt_AB), S_B(t)]
P_B(t) = w_A * t + w_A * Δt_BA + w_A * e_A + φ_A - w_B * t - w_B * e_B - φ_B

(22)

Here, PhaseCompare[S1, S2] calculates the phase shift (in radians) between two sine signals, S1 and S2.

Subtracting the outputs of the phase comparators, as derived from equations (21) and (22), yields:

ΔP(t) = w_A * Δt_BA - w_B * Δt_BA = (w_A - w_B) * Δt_BA = 2 * w * Δt (23)

Given that w_A = w_B = w and Δt_BA = Δt_AB = Δt, equation (23) simplifies to:

ΔP(t) = 2 * w * Δt (24)

Equation (24) signifies that the angle difference in the phase comparator outputs corresponds to twice the coaxial cable delay. Since the phase comparators essentially receive similar signals, their output subtraction effectively eliminates clock errors.

For a WUTI placed aboard a spaceship moving with velocity v and undergoing rotation by an angle α (as shown in Figure 7), equations (11) and (24) yield:

(ΔP(α)) / w = 2 * L / c^2 * v * sin(α) (25)

Similarly, for a WUTI situated on a spaceship orbiting a mass M at a distance r and rotating by an angle α (as depicted in Figure 10), equations (18) and (24) provide:

(ΔP(α)) / w = 2 * L / c^2 * √(2 * G * M / r) * sin(α) (26)

Equations (25) and (26) demonstrate that the Witte-Ulianov Time Interferometer illustrated in Figure 11 can discern variations in the "flow of time" between the locations of the atomic clocks. Equation (24) enables the WUTI to measure time dilation effects in line with Special Relativity, while equation (26) facilitates measurements aligned with the predictions of General Relativity. Each PC receive the signals defined by equations (19) and (20), also considering the delay in the coaxial cables. Considering that is the cable delay to the signal travel from point *X* to point *Y*, we can calculate:

$$P_A(t) = PhaseCompare[S_A(t), S_B(t + \Delta t_{BA})]$$
$$P_A(t) = w_A\, t + w_A\, e_A + \varphi_A - w_B t - w_B \Delta t_{BA} - w_B\, e_B - \varphi_B \quad (21)$$

$$P_B(t) = PhaseCompare[S_A(t + \Delta t_{AB}), S_B(t)]$$
$$P_B(t) = w_A\, t + w_A \Delta t_{BA} + w_A\, e_A + \varphi_A - w_B t - w_B\, e_B - \varphi_B \quad (22)$$

Where the *PhaseCompare*[S_1,S_2] function calculate the phase shift (in radians) from two sine signals S_1 and S_2 .

Subtracting the PCs outputs, from equations (21) and (22), give us:

$$\Delta P(t) = P_B(t) - P_A(t)$$
$$\Delta P(t) = w_A \Delta t_{BA} + w_B \Delta t_{AB} \quad (23)$$

Considering that:

$$w_A = w_B = w$$
$$\Delta t_{BA} = \Delta t_{AB} = \Delta t$$

Equation (23) becomes:

$$\Delta P(t) = 2w\Delta t \quad (24)$$

Equation (24) means that subtracting the PC output angle is equal to two times the coaxial cable delay. As the phase comparators receives basically the same signals, the subtractions of its outputs remove the clock errors.

If the WUIT presented at Figure 11 is placed at one spaceship moving at velocity *v* and rotating in an angle *α*, as defined in Figure 7, from equations (11) and (24) we can calculate:

$$\frac{\Delta P(\alpha)}{w} = \frac{2L}{c^2} v\, sin(\alpha) \quad (25)$$

If the WUIT presented at Figure 11 is placed at one spaceship orbiting the mass *M* at distance *r*, and rotating in an angle *α*, as defined in Figure 10, from equations (18) and (24) we can calculate:

$$\frac{\Delta P(\alpha)}{w} = \frac{2L}{c^2} \sqrt{\frac{2GM}{r}} sin(\alpha) \quad (26)$$

Equations (25) and (26) means that the Witte-Ulianov Time Interferometer presented at Figure 11, can detect “time flow” variations between the points where the atomic clocks are placed. Thus equation (24) allow the WUIT to measure time dilatation effects predicted by Special Relativity and equation (26) allow the WUIT to measure time dilatation effects predicted by General Relativity.

8. Wuti Implementation Using Two Laser Soucers:

Paul Dirac in his book "The Principles of Quantum Mechanics" has claimed quite famously that the interference of two independent light beams can never occur. He stated that "the wave function gives information about the probability of one photon being in a particular place, and not the probable number of photons in that place."

Nevertheless several published papers have shown that interference between two laser sources, seize presenting some technical complexities, can be performed [5-7].So, to achieve higher resolution the WUIT can use two laser sources as time references, replacing the atomic clocks and sine wave generators, meaning that the two signals to be “phase compared” becomes two laser beans,

The laser, phase comparing can be easy achieved using a bean splitter to merge the two laser beans, and the combined beam impinges on a photodetector as presented in Figure 12.

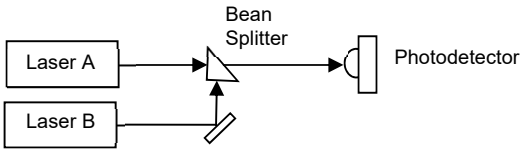

Figure 12: Two laser sources interference.

At the photodetector the light intensity I can be calculated from the laser beans equations:

$$E_A(r,t) = E_{0A}e^{i(k_A r - w_A t - \varphi_A)}$$
$$E_B(r,t) = E_{0B}e^{i(k_B r - w_B t - \varphi_B)}$$
$$I = (E_A + E_B)^2$$
$$I(r,t) = {E_{0A}}^2 + {E_{0B}}^2 - 2E_{0A}E_{0B}\,cos(\,(k_B - k_A)r - (w_B - w_A)t - (\varphi_B - \varphi_A))$$
$$I(0,t) = I_0 - I_1\,cos(\,\varphi_A - \varphi_B + tw_B - tw_A) \tag{26}$$

Equation (26), means that at the photodetector we can detect an wave with frequency proportional to the differences between the laser frequencies. So if we use laser sources with wave length very stable (or using light filters tuned to specific wavelengths, e. q. Farby-Perrot resonator) with few Hz difference between the operating frequencies, the photodetector output can be easy read to achieve the differences between the laser frequencies.

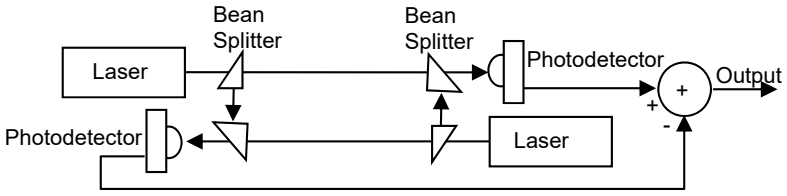

Figure 13: WUIT implementation using two Laser sources.

The Witte-Ulianov Time interferometer can be mounted using the Figure 12 optical configuration in two positions, as presented at Figure 13. For these configurations the intensity at each photodetector (I_A and I_B) can be calculated from equation (26), and the output signal (S), can be easy obtained subtracting these intensities:

$$I_A(t) = I_{0A} - I_{1A}\,cos(\,\varphi_A - \varphi_B + (t + \Delta t_{AB})w_B - tw_A)$$
$$I_A(t) = I_{0A} - I_{1A}\,cos(\,\phi + \Delta t_{AB}w_B) \qquad \Rightarrow \quad \phi = \varphi_A - \varphi_B + tw_B - tw_A$$
$$I_B(t) = I_{0B} - I_{1B}\,cos(\,\varphi_A - \varphi_B + tw_B - (t + \Delta t_{BA})w_A)$$
$$I_B(t) = I_{0B} - I_{1B}\,cos(\,\phi - \Delta t_{BA}w_A)$$
$$S(t) = I_B(t) - I_A(t)$$
$$S(t) = I_{0B} - I_{0A} + I_{1A}\,cos(\,\phi + \Delta t_{AB}w_B) - I_{1B}\,cos(\,\phi - \Delta t_{BA}w_A) \tag{27}$$

Considering that:

$$I_{0A} = I_{0B} = I_0$$
$$I_{1A} = I_{1B} = I_1$$
$$w_A = w_B = w$$
$$\Delta t_{BA} = \Delta t_{AB} = \Delta t$$

Equation (27) becomes:

$$S(t) = I_1(cos(\,\phi + w\Delta t) - cos(\,\phi - w\Delta t))$$
$$S(t) = -2I_{1A}\,sin(\,\phi)\,sin(\,w\Delta t)$$
$$S(t) = -2I_{1A}\,sin(\,\varphi_A - \varphi_B + tw - tw)\,sin(\,w\Delta t)$$
$$S(t) = -2I_{1A}\,sin(\,\varphi_A - \varphi_B)\,sin(\,w\Delta t) \tag{28}$$

Using some optical adjust the system can be adjusted to obtain the maximum output value (φ_A-φ_B = π/2) and so equation (28) becomes:

$$S(t) = -2I_{1A}\, sin(w\Delta t) \qquad (29)$$

From equation (29) we can consider that the phase variation inS(t) is given by:

$$\Delta P = w\Delta t \qquad (30)$$

As the two photodetectors, in Figure 13 receives basically the same signals, equations (29) and (30) given us an value that is constant if the delay Δtis also constant.

If we consider that the system presented at Figure 13 is placed in a spaceship moving at speed *v*, over a rotating table that can be associated with an α angle as presented at Figure 7, the value of Δt changes in function of the α angle as defined in equation (11), and so equation (30), can be written as:

$$\Delta P(\alpha) = w\Delta t(\alpha)$$
$$\Delta P(\alpha) = wL\frac{v}{c^2} sin(\alpha) \qquad (31)$$

Note that equation (31) is basically the same equation (25), meaning that we can also use laser beans to measure variation on the time flow. Thus, the WUIT that use atomic clocks (Figure 11) and the WUIT that use Laser sources as time reference sources have the same behavior. Otherwise, the laser sources operating at frequencies from 10^4 to 10^5 times greater than a sine wave generator frequency and allowing better accuracy to measured the phase delays.

For example, using a 10Mhz SG and considering that the phase comparator use 16bits Analogical Digital Conversers (ADC), given at least 10.000 levels to the phase detection processing, the WUTI time resolution is in order to 10^{-14}s.

If we use a He-Ne laser source (632nm wavelength), and considering that the photodetector output can be digitalized by an 16bits ADC, the time resolution of this WUTI is in order of $2x10^{-19}$s.

9. Exeriments Using Two Laser Soucers:

The author found, some experiments that confirm the possibility of measure the Witte effect using two laser sources. The first experiment performed in 1963 used two He-Ne laser placed in a rotting table as presented in Figure 14. The laser frequency difference was found to be constant to within 30Hz over times as short as about one second [8].

Figure 15 presents the frequency variation between lasers when the table is in rotation, resulting in 275 KHz sine wave, that this author believe appear in function of the Witte effect over the two laser sources.

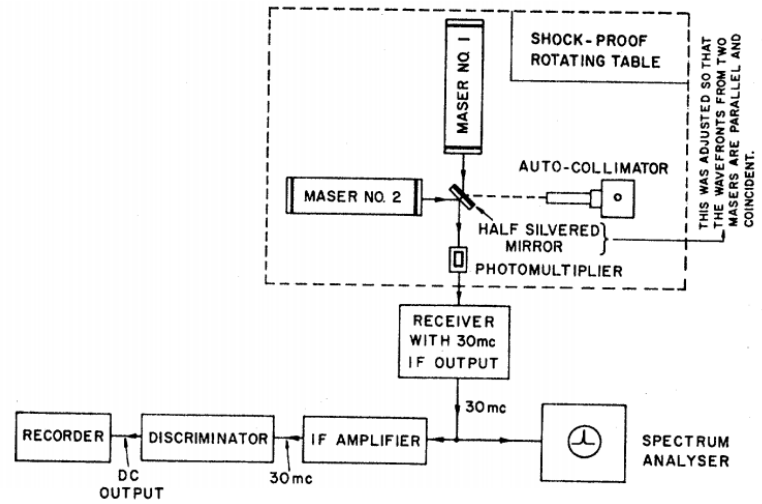

Figure 14: Schematic diagram for recording the variations in beat frequency between two optical maser oscillators when rotated through 90o in space. Apparatus on the shock-proof rotating table is acoustically isolated from the remaining electronic and recording equipment.

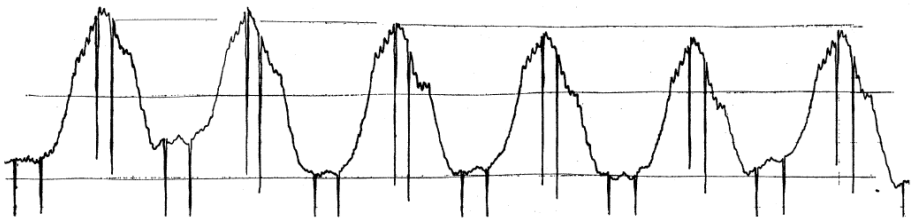

Figure 15: A plot of frequency variation between lasers due to 90o rotation of the table. Vertical scale is such that maximum variation is about 275 kHz. Markers indicate rotational angular positions zero and 90 o. Double markers appear because the total rotation slightly overshot the zero and 90' positions on each swing.

In the article we can see the flowing explanation for the 275 kHz signal, presented in Figure 15:

"The magnitude of this frequency change is about 275 kHz, or somewhat less than that attributable to the earth's orbital velocity on the simple ether theory. The change is mostly associated, as indicated above, with local effects such as the Earth's magnetic field, and must be measured throughout some appreciable part of the day to allow detection of any more fundamental spatial anisotropy."

The above explanation supposing that the *"Earth's magnetic field"* can change the laser frequencies was used, to not admit that some unknown effect is acting over the system. This author believes that the Witte effect can explain this frequency change, and so calculate its value from some parameter of this experiment.

The equation (29) developed to the laser configuration presented at Figures 12 and 13, cannot be applied to the system presented in Figure 14, because the lasers sources not are placed in the same line. Thus we need develop new equations to represent the Figure 14 system:

$$E_A(t) = E_{0A}e^{i(\varphi_A - w_A t)}$$
$$E_B(t) = E_{0B}e^{i(\varphi_B - w_B t)}$$
$$I = (E_A + E_B)^2$$
$$I(t) = {E_{0A}}^2 + {E_{0B}}^2 - 2E_{0A}E_{0B}\,cos(\,(\varphi_B - \varphi_A) - (w_B - w_A)t)$$
$$I(t) = I_0 - I_1\,cos(\,\varphi_0 + t(w_A - w_B))$$
$$I(t) = I_0 - I_1\,cos(\,\varphi_0 + \Delta w\, t) \qquad (32)$$

Knowing that w_A and w_B values depends on the laser wave length (λ_A and λ_B), considering the Earth speed (v) these lengths vary in function of the table rotation angle:

$$\lambda_A = \frac{w}{c}\sqrt{cos(\,\alpha)^2 + (1 - \frac{v^2}{c^2})\sin(\alpha)^2} \qquad (33)$$

$$\lambda_B = \frac{w}{c}\sqrt{sin(\,\alpha)^2 + (1 - \frac{v^2}{c^2})\cos(\alpha)^2} \qquad (34)$$

Thus for α equal to zero equations (33) and (34) given:

$$\lambda_A = \frac{w}{c}\ \ ;\ \lambda_B = \frac{w}{c}\sqrt{(1 - \frac{v^2}{c^2})}$$
$$w_A = c\lambda_A = w$$
$$w_B = c\lambda_B = \frac{w}{\sqrt{(1 - \frac{v^2}{c^2})}}$$
$$\Delta w = w_A - w_B = w(1 - \frac{1}{\sqrt{(1 - \frac{v^2}{c^2})}}) \qquad (36)$$

For α angle changing in 90º steps the frequency variations between the two lasers will have a maximum value that is like the same presented at equation (36). Thus, the equation (32) basically generates a sine wave whit maximum frequency that can be calculated by equation (36).

Otherwise, to obtain the signal generated from the laser interference, we need also consider the Witte effect acting over a distance L that is presented in Figure 16 as a red line contenting the centers of the laser sources.

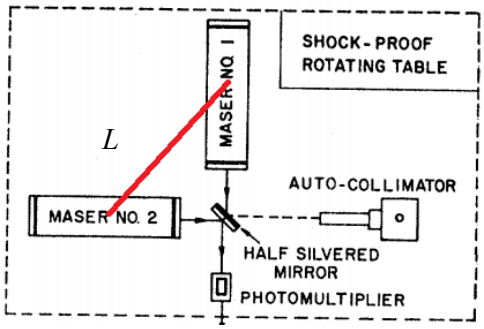

Figure 16: Distance L between the lasers sources, used to calculate the Witte effect.

If we consider the Earth moving in the space ate speed v, equation (31) allow calculate the Witte effect phase delay, given in radians. Otherwise, for the Figure 14 system, to convert the maximum phase delay (given in radians by equation (31)) in the maximum frequency variation (f , given in Hz), we need consider the sine wave signal defined in equation (32), which has an angular frequency Δw, using the flowing relation:

$$f = \frac{\Delta w}{\Delta P} \qquad (37)$$

Appling equation (36) to equation (37) give us:

$$f = \frac{\Delta w}{wL\frac{v}{c^2}} \qquad (38)$$

Knowing the laser frequency (w=1.88x10^{15} *rad/s*) and considering the Earth motion in relation the CMB (v=369 km/s), from equation (36) we can calculate:

$$\Delta w = 1.42\text{x}10^9 rad/s$$

Unfortunately, the article [8] does not have the physical dimensions of the experiment and is not possible to determine exactly the value of the distance L as presented in Figure 16.

Beside this we can suppose that L value can be found in a reasonable range, for example from 0.25m to 1.0m, and so obtained a range of values of frequency using equation (38):

$$L = 0.25m \ \Rightarrow\ f = 738kHz$$
$$L = 0.50m \ \Rightarrow\ f = 369kHz$$
$$L = 0.67m \ \Rightarrow\ f = 275kHz$$
$$L = 0.75m \ \Rightarrow\ f = 246kHz$$
$$L = 1.00m \ \Rightarrow\ f = 184kHz$$

Thus, if the distance between the laser centers in Figure 14, is in order to 67cm and considering the Erath speed in relation the CMB equal to 369km/h, applying the Witte effect to this system (equation (38)) give us an frequency variation in order of 275

kHz, that is the same measured at the experiment, as presented at Figure 15.

Other experiment was carried out in 1973, using two laser sources, as presented in Figure 17. This experiment use a He-Ne laser source placed at a rotating table and a CH4 stabilized laser in a fixed position acting as a reference source [9].

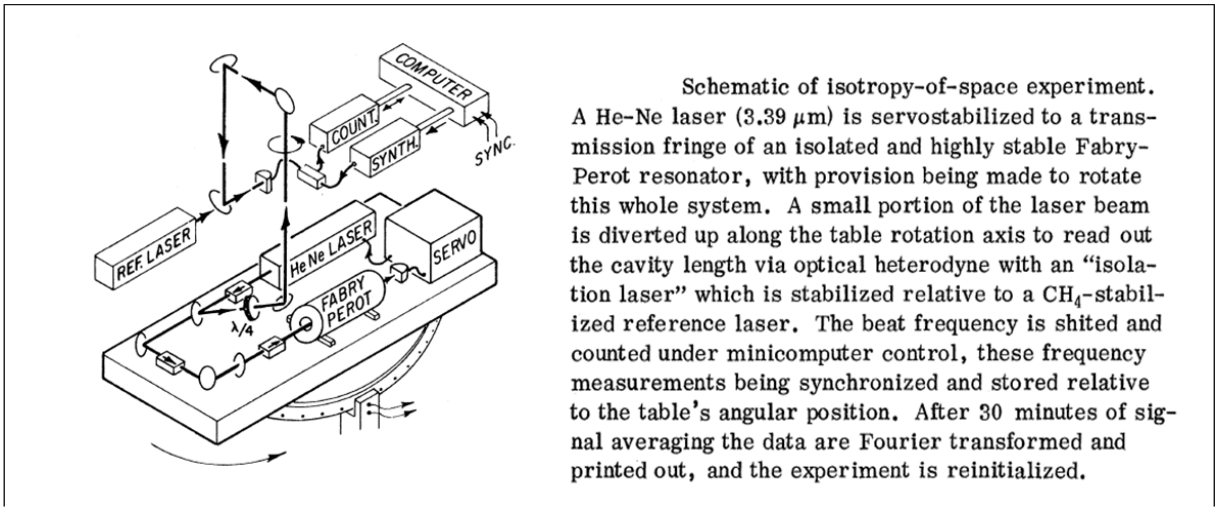

Schematic of isotropy-of-space experiment. A He-Ne laser (3.39 μm) is servostabilized to a transmission fringe of an isolated and highly stable Fabry-Perot resonator, with provision being made to rotate this whole system. A small portion of the laser beam is diverted up along the table rotation axis to read out the cavity length via optical heterodyne with an "isolation laser" which is stabilized relative to a CH_4-stabilized reference laser. The beat frequency is shited and counted under minicomputer control, these frequency measurements being synchronized and stored relative to the table's angular position. After 30 minutes of signal averaging the data are Fourier transformed and printed out, and the experiment is reinitialized.

Figure 17: Experiment using a rotation laser and a fixes laser.

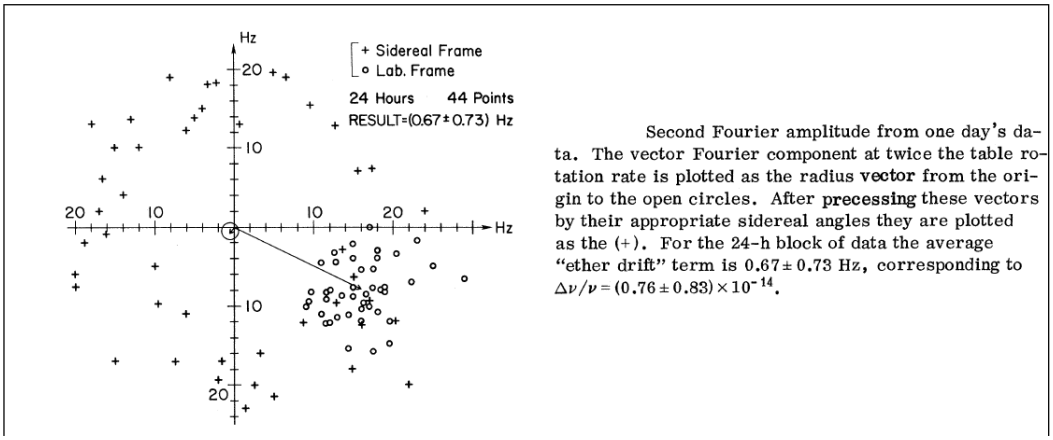

Second Fourier amplitude from one day's data. The vector Fourier component at twice the table rotation rate is plotted as the radius vector from the origin to the open circles. After precessing these vectors by their appropriate sidereal angles they are plotted as the (+). For the 24-h block of data the average "ether drift" term is 0.67 ± 0.73 Hz, corresponding to $\Delta\nu/\nu = (0.76 \pm 0.83) \times 10^{-14}$.

Figure18: Result from Figure 17 experiment.

It should be noted that the use of two laser sources generating interference patterns that can be easily observed and thus the Witte effect can be monitored by means of atomic clocks can also be measured using light sources having stable frequency.

10. Wuti Gravitacional Waves Observer:

The Witte-Ulianov Time interferometer can observe "time flow" variation predicted in Special Relativity for bodies moving in high speed and so "time flow" variation predicted in General Relativity for bodies inside strong gravitational fields.

This author believe that the WUTI can also detect gravitational waves.

Observing the WUTI "one arm" structure presented in Figure 11 that use two atomic clocks. Supposing that a gravitational-wave pulse "hit" the Clock A, it will affected by one time dilatation effect that initially not is observed over Clock B. As the gravitational-wave pulse travel at light speed, some microseconds after it "hit" clock B that will also be affected by the time dilatation. Thus the time delay between the two clocks varying with the gravitational wave and so the phase compares present complementary variations that can be observed at the WUIT output.

From equation (26) we can deduce that the WUIT output has a signal that is proportional to the gravitational-wave amplitude:

$$\Delta P(t) = \frac{2wL}{c^2} GW(t) \qquad (39)$$

Equation (39) meaning that the WUTI sensibility is related to the interferometer length (L) and to the angular frequency (w). Thus one good option is applied "all in fiber" optics components, as presented in Figure 19, and use optical fiber cables to connected the laser sources.

This kind of WUIT can use fiber optics cable whit many kilometer of length, and so the photodetector output signal need be recorded by an data acquisition system whit a global time synchronization, for example by the GPS time.

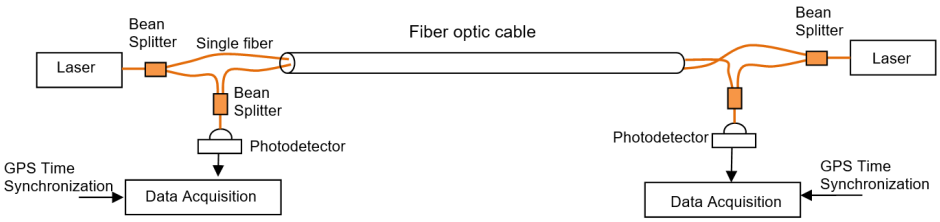

Figure 19: WUIT implementation using "all in fiber".

Figure 20 present, a "five arms" Witte-Ulianov Time interferometer, using the actual LIGO detector structure to implement the WUIT presented in Figure 13 and using the WUIT presented in Figure 19, to connect both installation,using a very long fiber optic cable (3.000 Km extension).

This kind of detector has the potential to observe gravitational waves, without low range frequency limitation and whit a large accuracy provides by the "all in fiber" WUIT that has the potential to be 1000 times more precise, because it is 1000 times longer.

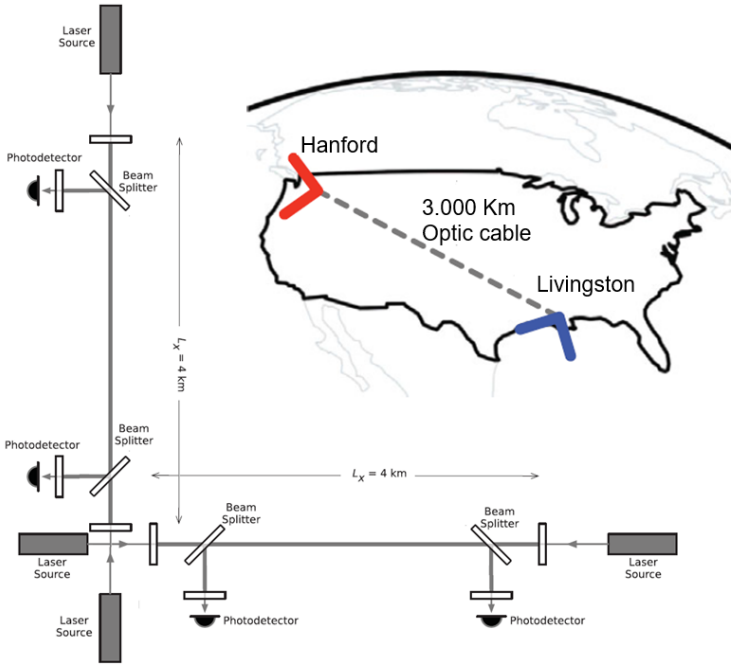

Figure 20: WUIT "five arms" implementation over the LIGO detectors.

11. CONCLUSION:

As the LIGO detector can operate only in a narrow band of frequencies (from 80hz to 300hz) the LIGO, system becomes more a black hole collision detector than a generic gravitational-waves detector.

It should be remembered that, although those responsible for LIGO, won the Nobel Prize in 2017, the number of scientists who today question the results of the LIGO, gravitational wave detections, grows every day. For example, Dr. Andrew Jackson from LIGO dissenting team, at the Niels Bohr Institute in Copenhagen, Denmark, it's very clear when speaking:

"We believe that LIGO has failed to make a convincing case for the detection of any gravitational wave event,"

I believe that the scientists, will soon realize that LIGO is a FAKE and that this detector cannot detect gravitational waves, because the light is also affected by GWs [10-13].

Today many people think that actually, LIGO is only detecting noise, or else electromagnetic terrestrial or sidereal phenomena, that are affecting the United States Power Grid, and generating simultaneous effects (limited by the speed of light) on the both LIGO detectors, as we can see in [14-31].

*"The analyze of the data for the gravitational wave (GW) events observed in LIGO detectors, from the viewpoint of signal estimation, detection and interference mitigation, shown that the GW events, are buried in detector noise and that the GW channel in the LIGO detector does in fact pick up strong 60*n Hz electromagnetic interference (EMI) from power lines…. and external magnetic field, from astrophysical objects, can enter the GW channel through electrical power points and wires, in which case we may not see any correlated peaks in the magnetometer channel and may mistake this interference, as a GW signal.... In conclusion, the magnetic coupling function between the received signal with the template in both the GW channel and the magnetometer channel is unknown for high frequencies. Hence it is suggested that the detected LIGO GW signals be further*

studied independently, given that magnetic field cannot be ruled out as a candidate for the GW events. ..."

It is interesting to observe that the LIGO teams themselves, report the presence of correlated noises in the two detectors and noise bursts (Blips) that appear continuously in the interval of a few minutes, in each day of operation, and that can be easily confused with gravitational waves, if by chance they happen at close intervals of time in the two LIGO detectors [32-33].

"Blip glitches are short noise transients present in data from groundbased gravitational-wave observatories. These glitches resemble the gravitationalwave signature of massive binary black hole mergers. Hence, the sensitivity of transient gravitational-wave searches to such high-mass systems and other potential short duration sources is degraded by the presence of blip glitches. The origin and rate of occurrence of this type of glitch have been largely unknown. In this paper we explore the population of blip glitches in Advanced LIGO during its first and second observing runs. On average, we find that Advanced LIGO data contains approximately two blip glitches per hour of data. We identify four subsets of blip glitches correlated with detector auxiliary or environmental sensor channels, however the physical causes of the majority of blips remain unclear."

Oh yes! these bursts of noise happen thousands of times a year, in the two detectors, and they don't know, where it comes from or what they are…What would actually be, the probability that two of these noise surges, happened at the same window time (10 ms) in both detectors, without having any correlation over them in a time window of several years? Would it be, something really impossible, for this "Blips", to occur simultaneously, and generate a false GW detection alarm in the LIGO detector? But then, how come they won a Nobel Prize, basically for th e first GW event that they detected? From what is stated in the and articles, the LIGO team, itself knew that there was a Great chance of some GW detected at LIGO, was the result of "Blips" and noise Bursts.

Even so, the LIGO, leaders preferred to ignore these facts, and present to the whole World, the first detection of LIGO (the GW150914 event) as proof that not only the LIGO detector works well but as a unnecessary proof the Einstein's General Relativity Theory, also works well!

Aside the fact, that they was sure to win the Nobel prize, the LIGO leaders, spending millions of Dolars producing media and paying advertising costs at magazines, newspapers, on television and on Internet pages, around world, with amazing news of one GW detection, that had a high chances of being a false alarm.

Obviously, at this first detection moment, they needed to justify the work of ten thousands scientists, who have been projecting, constructing and operating the LIGO detectors for over 20 years, without any presentable result, and also they need to justify the billions of dollars that have already been spent on the LIGO project, and in this critical, situation even the Nobel prize, ends up being a small bonus, for the LIGO leaders, and not the main concern of them…

On other hand, the Witte-Ulianov Time Interferometer here presented, can detecting gravitational-waves in very low frequency, and as stated in the title of this article, this detector can first see the ocean (the gravitational fields sea of the Moon, the Sun and Galaxy), and then it can see and record, the gravitational waves

The first step to obtain this new kind of detector, is confirm the existence of the Witte effect, that can be achieved in simple experiment, with very low coast, using two atomic clocks, two phase compare detectors and some kilometers of coaxial cables, as presented on this article.

Can be noted, the that historical experiments using two laser sources are not conclusive and have not explained effects, that this author believes, are related to the Witte effect, something that until now has not been recognized widely in scientific means. This occur because, in 1991, when R. D. Witte accidentally discovery, the Witte effect, the experimental results was interpreted by Witte, as proofs that the Einstein´s Especial Relativity was wrong.

The Witte, radical positioning turned the Witte effect in a kind of "bad" science. Then always in 2006, when R. T. Cahill showed that Witte effect, can be explained using Einstein's relativity, the Witte effect, was accepted at this first time, but still something obscure because, it use the Earth travel speed through, space as a velocity parameter, pointing to some sort of Ether, that can generate an absolute speed reference.

On the other hand, if we look at the Witte effect considering the orbit of the earth around the sun (average speed of 30km/s), or considering the gravitational field caused by the sun (for a distance given by the average radius of the orbit) the WUIT output has the same value. This means that the large gravitational fields, generated from Milk Way, and near galaxies can define a reference frame, to the Earth velocity, used in equation (1) that define the Witte effect.

This author believes that experiments using independents time sources, whether two atomic clocks or two laser sources, have until, now been poorly understood, and in a sense the physical scientists "fled" of these problems, avoiding points that apparently generated conflict with the Einstein's Relativity Theories.

Otherwise as the Witte, experiment with atomic clocks is very easy and cheap to be repeated, it is important to establish, more fully, the fact that the Witte effect exists, and can detect the "flow time" variations between two space time points.

If the Witte effect exist, it can be used as base to construct the Witte-Ulianov Time Interferometer, that is based in flow time variations detection. For this author, time distortions, as predicted by Einstein's, Especial and General Relativity, is the key to construct gravitational-wave detectors that can operate in very low frequency, that can observe gravitational waves whit period of seconds, minutes or even hours.

On this way the Witte-Ulianov Time Interferometer besides allowing to observe low frequency gravitational-waves also makes it possible to observe the ocean of gravitational fields that surrounding the Earth. It can also be used, to a low coast, improving of the current LIGO detector (using tree lasers instead of one) and create a New LIGO, that in the future, can by capable of detecting Real gravitational waves, instead of Fake GW, like this is doing now [34-38].

REFERENCES

1. Abbott, B. P., Abbott, R., Abbott, T., Abernathy, M. R., Acernese, F., Ackley, K., ... & Cavalieri, R. (2016). Observation of gravitational waves from a binary black hole merger. Physical review letters, 116(6), 061102.
2. Anderson, W. G., & Balasubramanian, R. (1999). Time-frequency detection of gravitational waves. Physical Review D, 60(10), 102001. https://arxiv.org/pdf/gr-qc/9905023
3. Ulianov, P. Y. Rotating the Einstein's light clock, to explain the Witte Effect. A basis to make the LIGO experiment work. https://citeseerx.ist.psu.edu/
4. Cahill, R. T. (2006). The Roland De Witte 1991 experiment (to the memory of Roland De Witte).
5. Dirac, P. A. M. (1981). The principles of quantum mechanics (No. 27). Oxford university press.
6. Louradour, F., Reynaud, F., Colombeau, B., & Froehly, C. (1993). Interference fringes between two separate lasers. American Journal of Physics, 61(3), 242-245.
7. H. Paul. Interference between independent photons. Rev. Mod. Phys 58, 209-231.
8. Jaseja, T. S., Javan, A., Murray, J., & Townes, C. H. (1964). Test of special relativity or of the isotropy of space by use of infrared masers. Physical Review, 133(5A), A1221.
9. Brillet, A., & Hall, J. L. (1979). Improved laser test of the isotropy of space. Physical Review Letters, 42(9), 549.
10. A. Unzicker. (2019). Fake News from the Universe? Blog on line Telepoli. https://www.telepolis.de/features/Fake-News-from-the-Universe-4464599.html
11. P. Valev (2023). LIGO's Gravitational Waves : Fake, Not Illusion, Forum on line Space.com. https://forums.space.com/threads/ligos-gravitational-waves-fake-not-illusion.60301/
12. Brooks, M. (2018). Exclusive: Grave Doubts over LIGO's Discovery of Gravitational Waves. New Scientist.:https://www.newscientist.com/article/mg24032022-600-exclusive-grave-doubts-over-ligos-discovery-of-gravitational-waves/
13. Ulianov, P. Y. (2016). Light fields are also affected by gravitational waves! Presenting strong evidence that LIGO did not detect gravitational waves in the GW150914 event. Global Journal of Physics, 4(2), 404-421. https://vixra.org/abs/2308.0033
14. Ulianov, P. Y., Mei, X., & Yu, P. (2016). Was LIGO's Gravitational Wave Detection a False Alarm?. Journal of Modern Physics, 7(14), 1845. https://www.scirp.org/html/1-7502879_71246.htm
15. Mei, X., Huang, Z., Ulianov, P. Y., & Yu, P. (2016). LIGO Experiments Cannot Detect Gravitational Waves by Using Laser Michelson Interferometers—Light's Wavelength and Speed Change Simultaneously When Gravitational Waves Exist Which Make the Detections of Gravitational Waves Impossible for LIGO Experiments. Journal of Modern Physics, 7(13), 1749-1761.https://www.scirp.org/journal/paperinformation.aspx?paperid=70953
16. Chen, X., Xuan, Z. Y., & Peng, P. (2020). Fake massive black holes in the milli-hertz gravitational-wave band. The Astrophysical Journal, 896(2), 171. https://iopscience.iop.org/article/10.3847/1538-4357/ab919f/pdf
17. Lukanenkov, A. V. (2015, June). Experimental detection of gravitational waves. In Physical Interpretation of Relativity Theory: Proceedings of International Meeting (pp. 343-358).
18. Lukanenkov, A. V. (2016). What registered LIGO 14.09. 2015. Engineering Physics, 8, 64-73.
19. Lukanenkov, A. V. (2017). Experimental Confirmation of the Doubts about Authenticity of Event GW150914. Journal of Applied Mathematics and Physics, 5(02), 538. https://doi.org/10.4236/jamp.2017.52046
20. Lukanenkov, A. (2018, July). Objective doubts about the authenticity of the event GW150914. In Journal of Physics: Conference Series (Vol. 1051, No. 1, p. 012035). IOP Publishing. https://iopscience.iop.org/article/10.1088/1742-6596/1051/1/012035/pdf
21. Brooks, M. (2018). Wave goodbye?. New Scientist, 240(3202), 28-32. http://usuario.cicese.mx/~ovelasco/archivos/mfluidos/Brooks2018_GravitationalWaves.pdf
22. Alderamin. (2019).LIGO delivers merrily loud laser light detections. Science Blogs: https://scienceblogs.de/
23. Collins, H. (2018). Gravity's kiss: The detection of gravitational waves. MIT Press.
24. Creswell, J., Von Hausegger, S., Jackson, A. D., Liu, H., & Naselsky, P. (2017). On the time lags of the LIGO signals. Journal of Cosmology and Astroparticle Physics, 2017(08), 013. https://arxiv.org/pdf/1706.04191
25. Naselsky, P., Jackson, A. D., & Liu, H. (2016). Understanding the LIGO GW150914 event. Journal of Cosmology and Astroparticle Physics, 2016(08), 029. https://arxiv.org/pdf/1604.06211.pdf
26. Liu, H., & Jackson, A. D. (2016). Possible associated signal with GW150914 in the LIGO data. Journal of Cosmology and Astroparticle Physics, 2016(10), 014. https://arxiv.org/pdf/1609.08346
27. Creswell, J., Liu, H., Jackson, A. D., von Hausegger, S., & Naselsky, P. (2018). Degeneracy of gravitational waveforms in the context of GW150914. Journal of Cosmology and Astroparticle Physics, 2018(03), 007. https://arxiv.org/pdf/1803.02350
28. Liu, H., Creswell, J., Von Hausegger, S., Jackson, A. D., & Naselsky, P. (2018). A blind search for a common signal in gravitational wave detectors. Journal of Cosmology and Astroparticle Physics, 2018(02), 013. https://arxiv.org/pdf/1802.00340
29. Liu, H., Creswell, J., von Hausegger, S., Naselsky, P., & Jackson, A. D. (2019). The role of redundancy in blind signal estimation for multiple gravitational wave detectors. International Journal of Modern Physics D, 28(04), 1930009. https://www.worldscientific.com/doi/pdf/10.1142/9789811258251_0006
30. Moorthy, C. G., Sankar, G. U., & RajKumar, G. (2017). LIGOs Detected Magnetic Field Waves; not Gravitational Waves. Imperial Journal of Interdisciplinary Research,

3(8), 268-269. https://www.academia-LIGOs_Detected_Magnetic_Field_Waves.pdf
31. Raman, A. (2018, November). ON SIGNAL ESTIMATION, DETECTION AND INTERFERENCE MITIGATION IN LIGO. In 2018 IEEE Global Conference on Signal and Information Processing (GlobalSIP) (pp. 1086-1090). IEEE.
32. Thrane, E., Christensen, N., & Schofield, R. M. (2013). Correlated magnetic noise in global networks of gravitational-wave detectors: observations and implications. Physical Review D, 87(12), 123009. https://link.aps.org/accepted/10.1103/PhysRevD.87.123009
33. Cabero, M., Lundgren, A., Nitz, A. H., Dent, T., Barker, D., Goetz, E., ... & Davis, D. (2019). Blip glitches in Advanced LIGO data. Classical and Quantum Gravity, 36(15), 155010. https://iopscience.iop.org/article/10.1088/1361-6382/ab2e14/ampdf
34. Benton, C. P. Einstein's Theory of Special Relativity Made Relatively Simple. http://docbenton.com/relativity.pdf
35. Frolov, V., & Novikov, I. (2012). Black hole physics: Basic concepts and new developments (Vol. 96). Springer Science & Business Media.
36. Ulianov, P. Y. Witte-Ulianov Rotation Anisotropy Effect Rotating the Einstein's light clock, to show that the neutrinos travel at the light speed in OPERA and MINOS experiments. https://citeseerx.ist.psu.edu/
37. Steltner, B., Papa, M. A., Eggenstein, H. B., Allen, B., Dergachev, V., Prix, R., ... & Kwang, S. (2021). Einstein@ Home all-sky search for continuous gravitational waves in LIGO O2 public data. The Astrophysical Journal, 909(1), https://iopscience.iop.org/article/10.3847/1538-4357/acdad4/pdf
38. Nielsen, A. B., Nitz, A. H., Capano, C. D., & Brown, D. A. (2019). Investigating the noise residuals around the gravitational wave event GW150914. Journal of Cosmology and Astroparticle Physics, 2019(02), 019. https://arxiv.org/pdf/1811.04071